REMOTE MONITORING OF DAILY CHANGES IN CARDIAC MECHANICAL EFFICIENCY AND OTHER CARDIAC PARAMETERS IN A COASTAL KAYAKER OVER ONE-MONTH OF PADDLING

ISSN 1590-8844
International Journal of Mechanics and Control, Vol. 26, No. 02, 2025
https://doi.org/10.69076/jomac.2025.0028

REMOTE MONITORING OF DAILY CHANGES IN CARDIAC MECHANICAL EFFICIENCY AND OTHER CARDIAC PARAMETERS IN A COASTAL KAYAKER OVER ONE-MONTH OF PADDLING

FilippoTocco[1,10], Giovanna Ghiani[1], Marco Palmas[1,10], Michele Ruggiu[1,10], Fernanda Velluzzi[1], Deledda A[1], Alberto Masala[2], Andrea Fois[3], Andrea Manuello Bertetto[4], Antonio Hector dell'Osa[5], Angelo Cerina[6], Cristiana Cappagli[7], Salvatore Melis[1,8,10], Valentina Loi[9], Ricardo Marcello[9], Alberto Concu[9,10]

[1]Department of Medical Sciences and Public Health, University of Cagliari, Italy
[2]Sports Medicine Association of Sassari, Sassari, Italy
[3]Nomadyca Ltd, Remote Biosignals Acquisition Unit, Mulago Hospital, Kampala, Uganda
[4]Department of Mechanical and Aerospace Engineering, Politecnico di Torino, Turin, Italy
[5]Laboratorio de Electrónica Aplicada y Biomedicina, Universidad Nacional de Tierra del Fuego, Ushuaia, Argentina
[6]Acquaforte Thalasso & Spa Medical Team, Forte Village Resort, Santa Margherita di Pula, Cagliari, Italy
[7]Kpurple, individual company, Cagliari, Italy
[8]Sardinia's Schools Direction Office, Physical and Sports Education Unit, Ministry of Education and Merit, Cagliari, Italy
[9]AC Technologies Ltd, Internet of Things Unit, Cagliari, Italy
[10]Sporting Life & Medicine Lab, Sardegna Ricerche, Cagliari, Italy

ABSTRACT

A male kayaker covered approximately 1,000 km along a sea coast over a period of ~40 days. Each night, after setting up camp, he noninvasively self-recorded at rest several systemic variables and transmitted them to a remote medical center via a telemedicine platform developed by the research team. This system employed a custom-built wearable device based on electrical impedance to acquire beat-to-beat cardiodynamic variables. Additional measurements included arterial blood pressure, expiratory peak flow, maximal handgrip force, tympanic temperature, and urine specific gravity. Over the course of the expedition, cardiac output linearly increased by 65 ml min^{-1} per day, primarily due to a rise in stroke volume and a concomitant reduction in total peripheral vascular resistance which, in turn, led to a decrease in mean arterial pressure. The mechanical work of the heart showed no significant variation during navigation. However, towards the end of the journey, the rate–pressure product—an indicator of myocardial oxygen consumption—rose exponentially, indicating a progressive decline in cardiac mechanical efficiency. This trend paralleled a decrease in maximal handgrip strength and an increase in perceived exertion. Overall, the kayaking expedition promoted an improvement in oxygen delivery capacity and blood pressure lowering, although signs of cardiac and muscular fatigue became evident toward the end of the trip.

Keywords: kayaking, cardiodynamics, remote data assessing, heart mechanical efficiency

1 INTRODUCTION

Nautical motion activities performed with a paddle, i.e. kayaking, are characterized a motor pattern that leads to the activation of numerous muscle groups. Specifically, to execute the technical paddling movement—which primarily involves the muscles of the arms and shoulders—the paddler also engages the muscles of the back responsible for trunk rotation, as well as the core muscles, including the abdominals, which contribute to maintaining balance and proper spinal alignment. The legs are likewise involved, as they are subjected to a condition of isometric hypertonia during motion-specific performance. Therefore, kayak-specific functional training integrates aerobic conditioning —to enhance endurance—with muscular strengthening and toning, aimed at improving overall performance. From a biomechanical standpoint, kayak technique is a cyclical

Contact authors: Filippo Tocco[1], Alberto Concu[2]
[1]Dept of Medical Sciences and Public Health, University Cittadella, Provincial Road 8 – 09042 Cagliari, Italy
[2]AC Technologies Ltd, Internet of Things Unit, Via Pais 12- 09128 Cagliari, Italy
E-mail: aconcu44@gmail.com, filippo.tocco@tiscali.it

movement characterized by alternating right- and left-side strokes. During each stroke, the kayak exhibits fluctuations in acceleration because the paddler's dynamic motion, together with the varying magnitudes of propulsive and resistive forces, gives rise to oscillations in boat velocity. Consequently, the ability to achieve a high stroke rate is inversely proportional to stroke duration, such that greater kayak speed can be attributed to an increased stroke frequency. With the aim of investigating the systemic adaptations that characterise the body's response to long-duration physical activity training in a kayak carried out in a coastal marine environment, in a male kayaker who covered approximately 1,000 km along the coast over ~40 days, maximal kayak-ergometer tests to exhaustion after the trip has been found that VO_2peak normalized to body mass increased by 13%, the respiratory exchange rose by 16%, and estimated energy expenditure increased by 12%. Moreover, in this athlete echocardio-graphic assessment revealed a 32% increase in resting left ventricular stroke volume following the trip [1]. Since during his coastal voyage, this athlete was able each night—after dinner and after making camp—to noninvasively at rest self-record several systemic variables and transmit them to a remote specialized medical centre (RSMC) using a telemedicine device developed by the research team [2], in this study, it has been investigated the daily adjustments in the engagement of the athlete's physiological systems induced by paddling. This approach elucidated the time-dependent intrinsic adaptations underlying the morpho-functional changes that were previously observed following completion of the trip [1].

2 METHODS

2.1 THE SUBJECT AND HIS KAYAK

The participant was a highly skilled 47-year-old male kayaker who served as a federal-level rowing instructor at an Italian sports club. He frequently undertook long coastal kayak trips for both athletic and recreational/touristic purposes. For this study he circumnavigated the island of Sardinia (Italy) by kayak (Diana Canoe Manufacturers, model 535), covering 969 km over 41 days (see Figure 1). After each day of paddling he searched for a coastal site in which to camp overnight; if weather conditions precluded further navigation, he sometimes sheltered during the day as well. These circumstances resulted in prolonged stops during the trip, sometimes lasting several days.

2.2 INSTRUMENTATION

As shown in Figure 1, a flexible photovoltaic panel (Energy Flyer, Solbian, Turin, Italy) was installed on the stern of the boat; its specifications are reported in Figure 2. The compact panel weighs 360 g and which comprises four solar cells, delivering a maximum power of 12.5 W and a maximum current of 2.4 A at a nominal voltage of 5 V. While the kayak was underway and exposed to sunlight, the Energy Flyer panel charged a power bank via a standard USB port.

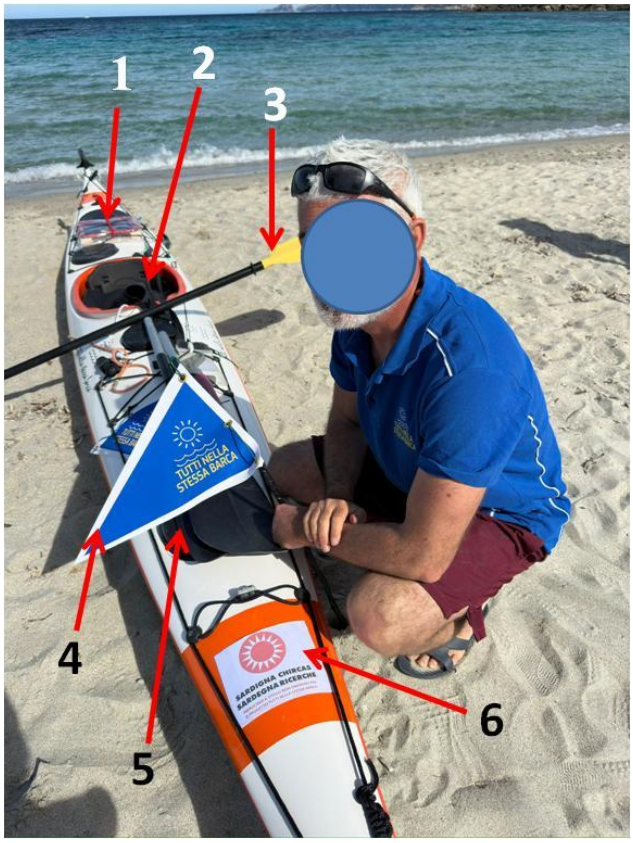

Figure 1 The kayak and its kayaker. (1) photovoltaic panel; (2) cockpit; (3) paddle; (4) pennant bearing the expedition name; (5) watertight bow locker containing scientific instruments; (6) adhesive panel bearing the logo of Sardegna Ricerche, the Italian research institution that provided patronage for the experiments together with the Polytechnic University of Turin in Italy.

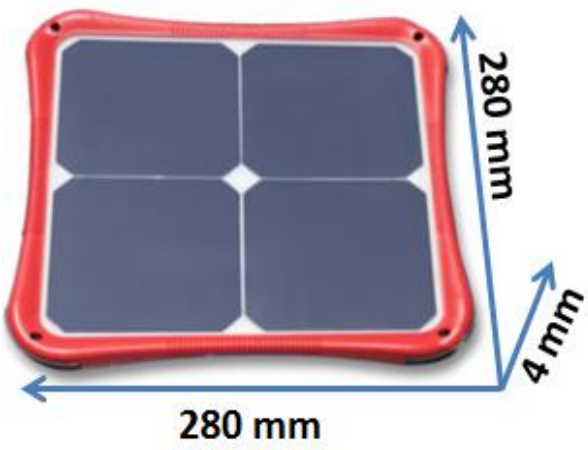

Figure 2 The flexible, square photovoltaic panel (model Energy Flyer) mounted on the stern of the kayak. Its three spatial dimensions—length, width, and thickness—are indicated by blue axes, with values shown in millimetres (mm). A protective red rubber frame with one anchoring hole at each corner surrounds the panel's active area, which consists of four black photovoltaic cells.

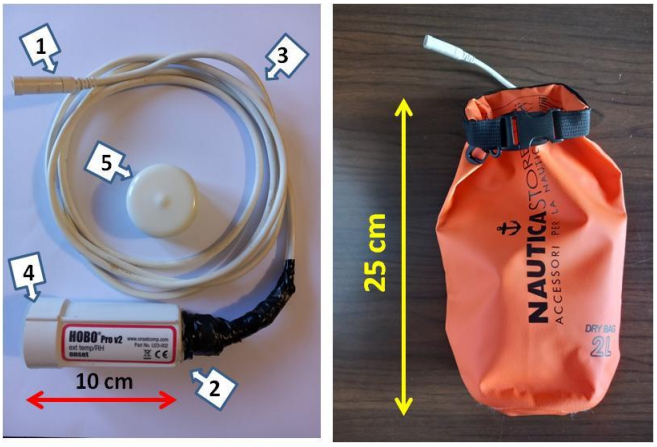

Figure 3 On the left a photo of the sensing device to record environment's temperature and humidity. 1) sensors tip, 2) device body with dedicated electronics for data recording, 3) 175 cm long connection cable between the tip and the body of the device, 4) optical emitter interface for the transmission of the stored signals, 5) protective cap of the optical interface. On the right the closed waterproof nautical bag from which only the sensorized head emerged.

The power bank then supplied power to the electronic devices used for functional measurements once the kayaker landed to set up the night camp. During navigation, all equipment was enclosed in a waterproof casing that was transparent to sunlight. The kayak was also fitted with a waterproof data logger (HOBO Pro v2, LI−COR, Lincoln, USA) shown in Figure 3 that recorded ambient air temperature (*°C*) and relative humidity (%) at 30−second intervals. The logger was housed in a 2 litter waterproof nautical bag with only the sensor tip protruding, and was secured daily in the cockpit by attaching it to the sides of the seat. Upon disembarking, the athlete brought the bag containing the HOBO into the overnight camp to enable a continuous 24-hour recording. Instrumental traces in Figure 4 illustrate a representative day of these measurements. When inserted into a splash−resistant docking station, this interface permits data transfer from the HOBO logger via an optical USB connection.

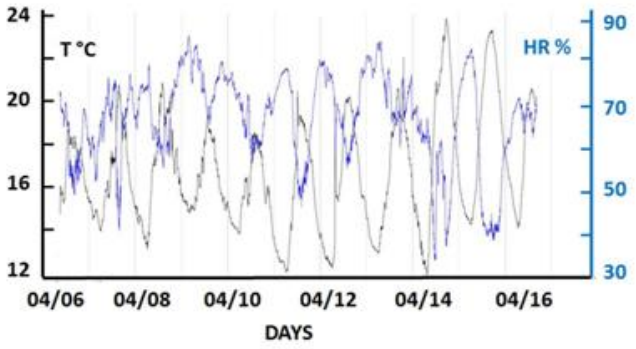

Figure 4 Time series of environmental temperature (T, *°C*; black) and relative humidity (RH %; blue) recorded by the HOBO logger from 6 to 16 April. Both the lowest temperatures and highest relative humidity were observed at night.

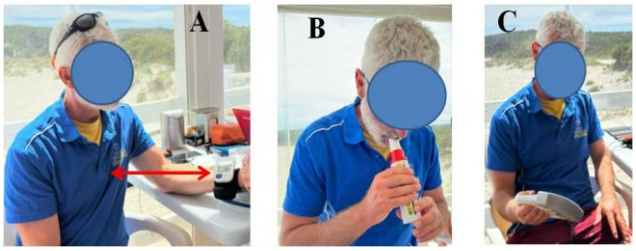

Figure 5 Photographs illustrate examples of the kayaker performing daily physiological measurements after landing: (A) arterial blood pressure measured with an automatic wrist sphygmomanometer, ensuring that the device was kept at heart level (indicated by the double red arrow); (B) peak expiratory flow assessed using a graduated tube inserted into the mouth and held with both hands, taking care not to obstruct the sliding cursor along the scale (*l min^{-1}*) and (C) handgrip strength measured with the dominant hand using a dynamometer, displaying the maximum contraction force in *kg* on its screen.

Inside a waterproof nautical bag stored in the kayak's bow locker (see Figure 1), the athlete kept the equipment used to self-record noninvasive data, which he transmitted to the RSMC each night after dinner and after establishing camp. The instrumentation included:

- a custom-built wearable device [3] for acquiring thoracic electrical impedance (Zt in Ω), which reciprocal also represents the thoracic fluid index (TFI in Ω-1), enabled the use of impedance cardiography (ICG) to non invasively obtain beat-to-beat cardiodynamic variables together with an ECG trace (E-Physio Tool, AC Technologies Ltd, Cagliari, Italy), the device requires a 5 V DC power supply capable of deliver 2A.
- a miniaturized automatic wrist sphygmomanometer (Omron HEM-6181, Kyoto, Japan), shown in Figure 5, was used to acquire systolic (SABP) and diastolic (DABP) arterial blood pressures (in *Torr*) together with heart rate (HR; bpm), the device has been validated
- according to the ANSI/AAMI/ISO 81060-2:2013 protocol [4];
- a manual device for measuring peak expiratory flow (PEF), expressed in l min-1, which consisted of a graduated cylinder to be inserted into the mouth through into which the subject performed a maximal forced;
- exhalation (Mini-Wright, Clement Clarke International, UK) (see Figure 5) [5];
- a device for assessing maximal force output during the handgrip maneuver (HAG), measured in kg and performed with the dominant hand (Gripx, Vatmaster Consulting, Germany), is shown in Figure 5 [6];
- a fingertip pulse oximeter (Pheartcare; Shenzhen Lepu Intelligent Medical Equipment Ltd., Shenzhen, China) was used to measure beat-to-beat arterial blood oxygen saturation (SO2 %) [7];
- an electronic tympanic thermometer (Gima, Italy) was chosen to measure Body temperature (BT) in °C [8];
- a tool to measure urine specific gravity (USG) through multifunction reagent strips (Combi Screen, Germany) [9].

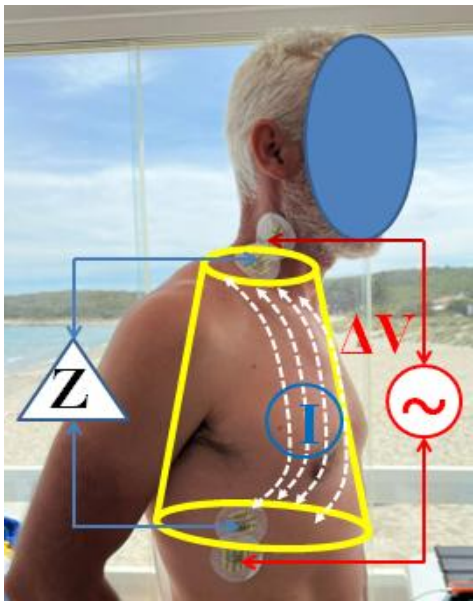

Figure 6 Schematic representation of thoracic electrical bioimpedance assessment in the athlete's chest using the E-Physio Tool. The inverted cone-shaped trunk, shown in yellow, symbolically represents the volume of tissues contributing to the electrical impedance (VEPT). The smaller base of this anatomical solid lies at the level of the neck muscle roots, while the larger base corresponds to the plane of the xiphoid process. Two disposable electrodes are positioned on the right side of the neck and thorax (with four additional electrodes symmetrically placed on the left side). The outer electrodes, connected by red cables, are linked to the voltage generator (ΔV), whereas the inner electrodes, connected by blue cables, are linked to the impedance meter (Z). The impedance measurements dependon an electrical current (I) of 1 *mA* at 65 *kHz* passing through the thorax, represented here by white dotted lines.

All acquired functional data were transmitted via a proprietary information and communication technology (ICT) platform implementing the E-Physio Tool together with telemedicine software [2] to the RSMC, where experienced researchers performed detailed analyses.
The electronic and informatics characteristics of this ICT platform have been described extensively elsewhere [2,3,10–12]. Left ventricular stroke volume (SV) was therefore estimated on a beat-to-beat basis (*ml*) from the following variables directly derived from impedance measurements [13]:

- - left ventricular preload index (LVPLI), also called the central (cardiac) heterometric stroke-volume–modulating factor, defined as TFI (1/Zt, units: Ω^{-1});
- - left ventricular myocardial contractility index (LMCI), also called the central (cardiac) homeometric stroke-volume–modulating factor, defined as the ventricular peak systolic ejection velocity (EVI) (units: $\Omega\, s^{-1}$);
- - ventricular ejection time, defined as the interval between aortic valve opening and closing, which is directly related to SV (VET) (units: *s*).

According to the Sramek–Bernstein equation [14], a subject's SV can be estimated by the volume of thoracic tissues contributing to the impedance (VEPT, ml) [15] together with the three impedance-dependent variables described above. VEPT comprises all thoracic tissues contained within the geometric solid shown in Figure 6 and can be obtained from a dedicated nomogram that relates three variables—gender, body mass, and height—using a set of scales arranged so that the value of one variable is determined by drawing a straight line through the corresponding points on the other scales [14].
That following is the Sramek-Bernstein equation:

$$SV = VEPT\{ml\} * TFI\{\Omega^{-1}\} * EVI\{\Omega s^{-1}\} * VET\{s\} = ml \qquad (1)$$

Equation (1) is valid because, when the cardiovascular system is modelled as a simple closed hydraulic circuit with a reciprocating plunger pump in series (the heart), each suction–delivery cycle of the pump (diastole and systole respectively) yields multiplicative terms that correspond dimensionally to the electrical analogs of the four hydraulic variables that characterize the system. In this formulation, the volume ejected per pump cycle is directly related to the peak ejection velocity and the duration of ejection. Accordingly, the four variables on the right-hand side of (1) represent, respectively: the pump's hydraulic volume (blood volume) or VEPT; the suction volume or LVPLI (measured as TFI); the peak delivery velocity or LVMCI (measured as EVI); and the delivery duration or VET.

2.3 ESPERIMENTAL PROTOCOL

Due to unexpected atmospheric and technical problems at the start of the trip, remote acquisition of the daily data transmitted by our kayaker to the RSMC was delayed by 10 days. Consequently, the ICT platform's daily analysis covered the subsequent 31 days of the trip.
Beat-to-beat Zt and ECG data were acquired remotely on a daily basis while the athlete was seated and in a relaxed state for 3 minutes. Using the LabChart reader (ADInstruments, Oxford, UK) [16], a trained operator at the RSMC identified 10 consecutive heartbeats beginning 1.5 minutes into each recording. From each beat, the operator extracted LVPLI (TFI in Ω^{-1}), LVMCI (EVI in $\Omega\ s^{-1}$), ventricular ejection time (VET in s), and heart rate (HR in *beats* min^{-1}) from the R–R intervals.
At each selected heartbeat, the operator at the RSMC calculated the stroke volume (SV) by applying Equation (1), and subsequently derived the CO, expressed in $l\ min^{-1}$ as follows:

$$CO = SV * HR \qquad (2)$$

Furthermore, the mean ± standard deviation (M ± SD) of the ten measurements obtained for each variable (TFI, EVI, VET, SV, and CO), were computed. During the same experimental session, to avoid any emotional interference related to the temporal overlap with the subsequent impedance data collection, the athlete self-recorded SABP DABP at the wrist at the beginning of the 3-minute

impedance data acquisition period. After the 3 minutes of relaxation, the athlete proceeded with the remaining instrumental assessments, as described in Figure 5, and concluded with the SO_2%, SUG, and BT measurements. These manually recorded readings were transmitted to the RSRC via WhatsApp application, along with a self-reported rating of perceived exertion (RPE) for the same day, expressed on a 6–20 scale according to Borg's method [17]. From the data acquired on the same day at the RSMC, the mean arterial blood pressure (MABP) was calculated in *Torr* using the following equation:

$$MABP = [(SABP + 2*DABP) : 3] \quad (3)$$

The left ventricular afterload index (LVALI), also referred to as the peripheral heterometric modulator of SV, was estimated in terms of total peripheral vascular resistance (TPVR), calculated as:

$$TPVR = [MABP : CO] \quad (4)$$

and expressed in *Torr* l^{-1} min, considering that the CO value used corresponds to the average of ten cardiac beats. Further, rate–pressure product (RPP), an index of cardiac oxidative energy expenditure [18], was determined as:

$$TPVR = [MABP : CO] \quad (5)$$

and expressed in *Torr beats* min^{-1}.
The heart mechanical work index (HMW) [8] was computed as:

$$HMW = [SV * MABP] \quad (6)$$

expressed in *ml Torr*.
Finally, the heart mechanical efficiency index (HME) [8] was obtained as:

$$HME = [HMW : RPP] \quad (7)$$

and expressed in *ml min beats* $^{-1}$.
Both descriptive and predictive statistics were used, including linear and quadratic regression analyses. The model with the highest significance was selected. A P-value < 0.05 was considered as statistically significant.

2 RESULTS

Firstly, it should be noted that, in the x-axis of the following graphs, the time data refer to a 16-day period, with measurements taken every two days during the athlete's 31-day journey, as described in the Methods section. Table I reports the mean ± standard deviation (SD) of all cardiovascular variables derived from the beat-to-beat analysis of bioimpedance and ECG recordings obtained using the e-Physio Tool worn by the kayaker on 14 of the 16 days considered in this study. Data from two days were excluded due to electrical interference that prevented reliable impedance measurements. As indicated in the table, each reported value represents the average of 140 beats, corresponding to 10 consecutive beats selected within the 3-minute resting bioimpedance recording period. These recordings were acquired at the end of his daily physical activity before going to sleep.

Table I – Average values of beat-to-beat assessed cardiovascular variables

N (140)	TFI Ω	EVI Ω s^{-1}	VET ms	HR b min^{-1}	SV ml	CO l min^{-1}
Mean	32.5	1.89	373	64.4	62.9	4.19
±SD	3.2	0.5	31.8	8.9	14.6	1.43
VI%	9.8	26.4	8.5	13.8	23.2	34.1

TFI: bioimpedance index of thoracic fluids; EVI: left ventricle index of the blood ejection velocity peak; VET: left ventricle ejection time; HR: heart rate in beats (b) per minute; SV: left ventricle stroke volume; CO: cardiac output per minute; VI: variability index as SD percentage on Mean. N: number of considered beats to calculate average values (Mean) and its standard deviation (±SD).

Figure 7 shows the geometric representation of the linear regression of stroke volume (SV) across the selected days during which the tested athlete was engaged in the circumnavigation of Sardinia by kayak. The regression equation was that following:

$$SV\ (ml) = 55.97 + 1.22\ (days) \quad (8)$$

Equation (8) predicts that, over the course of the kayaking days, the athlete's resting SV increased by approximately 1.22 ml every two days. However, Equation (8) yielded a "P" value of 0.06, which was not statistically significant,

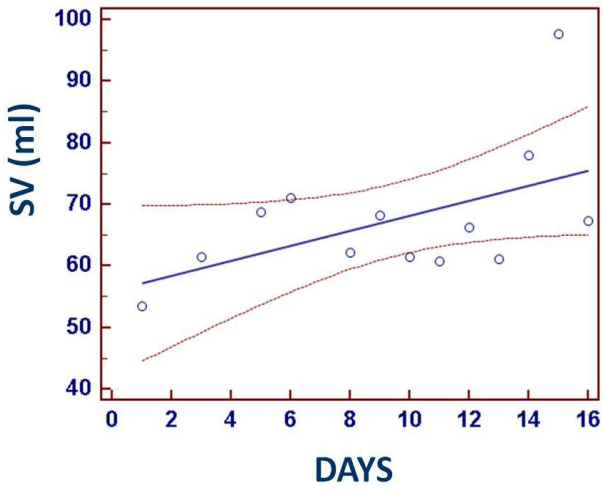

Figure 7 The linear regression of stroke volume (SV) values against the corresponding days of assessment, represented by a straight line fitted to 13 valid data points (open circles). One data point was excluded from the analysis as an outlier. The two orange dashed lines indicate the 95% confidence interval.

although it was close to the threshold of $P < 0.05$ adopted in this study as the criterion for significance. The following regression equations best describe the relationships between the preload index TFI, i.e. 1/Zt, (8) and the contractility index EVI (10) of the left ventricle over the tested days of cruising, as graphically illustrated in Figures 8 and 9, respectively.

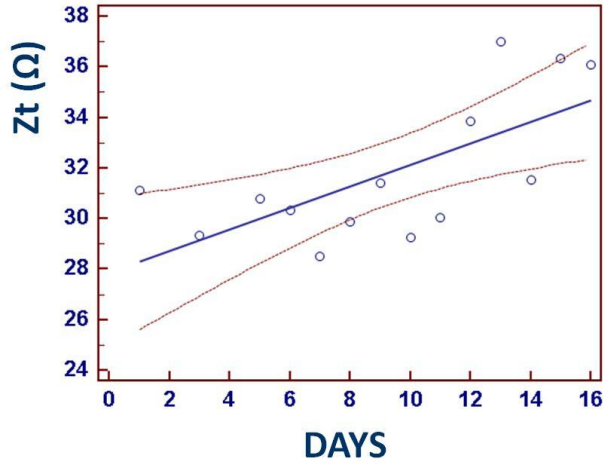

Figure 8 The linear regression of Zt values (the reciprocal of TFI, representing preload) plotted against the corresponding days of assessment. The regression is depicted as a straight line segment with 14 open circles indicating the accepted measurements. The two orange dashed lines represent the 95% confidence interval.

Each of these indices, as is well established, contributes to the central (cardiac) regulation of SV through heterometric and homeometric mechanisms, respectively.

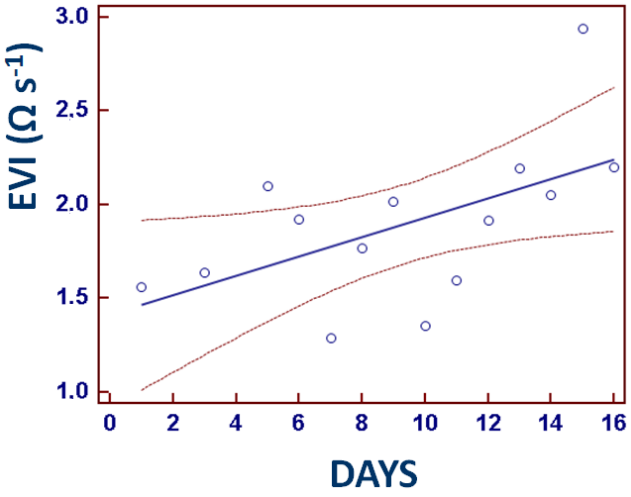

Figure 9 shows the linear regression of EVI values (contractility index) plotted against the corresponding days of assessment. The regression is depicted as a straight line segment with 13 open circles indicating the accepted measurements, as one data point was excluded due to being identified as an outlier. The two orange dashed lines represent the 95% confidence interval.

$$Zt\ (\Omega) = 27.89 + 0.42\ (days) \quad (9)$$

$$EVI\ (\Omega\ s^{-1}) = 1.416 + 0.052\ (days) \quad (10)$$

Both Equations (9) and (10) represent linear regressions that reached statistical significance ($P = 0.007$ and $P = 0.037$, respectively). In contrast, the linear ($P = 0.161$) and quadratic ($P = 0.209$) regression models describing the relationship between HR and the 14 days of paddling did not achieve statistical significance. Nevertheless, this relationship is illustrated graphically in Figure 10.

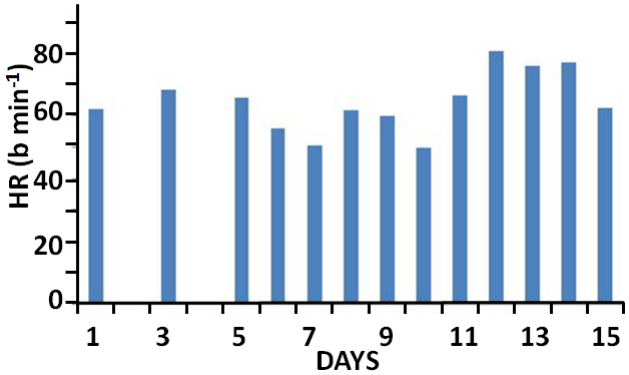

Figure 10 A column histogram showing the heart rate (HR, beats per minute) for each of the 13 selected days out of the 16 days of kayaking.

As previously described in the Methods section, data from days 2 and 4 were excluded from the analysis, while day 16 was identified as an outlier. E-Physio Tool. These measurements were recorded simultaneously with the impedance assessments and, in some cases, were mathematically integrated with the corresponding averaged impedance-derived values, as clearly described in the Methods section. Although the HR regressions shown were not statistically significant, the linear regression of CO over the 14 selected days (Figure 10) was:

$$CO\ (l\ min^{-1}) = 3.35 + 0.13\ (days) \quad (11)$$

Table II reports the mean ± SD values of cardiovascular variables obtained from different devices, in addition to the

Table II – Non-impedance deriving cardiovascular variables

N (13)	MABP Torr	TPVR Torr ml^{-1} min	RPP beats min^{-1} Torr	HMW ml Torr	HME beats^{-1} min ml
Mean	82.9	18.9	7574.5	5225.4	0.75
±SD	9.1	9.8	674.1	936.1	0.13
VI%	11.0	51.8	8.9	17.9	17.3

MABP: mean arterial blood pressure; TPVR: total peripheral vascular resistance; RPP: rate–pressure product; HMW: heart mechanical work; HME: heart mechanical efficiency; VI: variability index, expressed as the percentage of the standard deviation relative to the variable mean. N indicates the total number of measurements considered for calculating the mean value (Mean) and its corresponding standard deviation (±SD).

which yielded a "P" value of 0.017, thus reaching statistical significance. Figure 11 shows the linear relationship between MABP and the selected days.
The corresponding regression equation was:

$$MABP\ (Torr) = 91.28 - 1.19\ (days) \quad (12)$$

Equation (12) yielded a "P" value of 0.009, indicating statistical significance. Figure 13 shows the linear inverse regression of TPVR over the selected days.

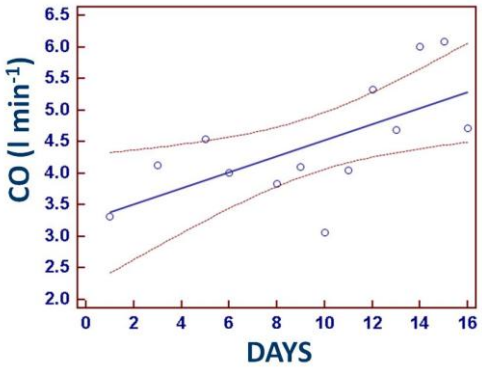

Figure 11 The linear regression of cardiac output (CO) values plotted against the corresponding days of assessment. The regression is depicted as a straight line segment with 13 open circles indicating the accepted measurements, as one data point was excluded after being identified as an outlier. The two orange dashed lines represent the 95% confidence interval.

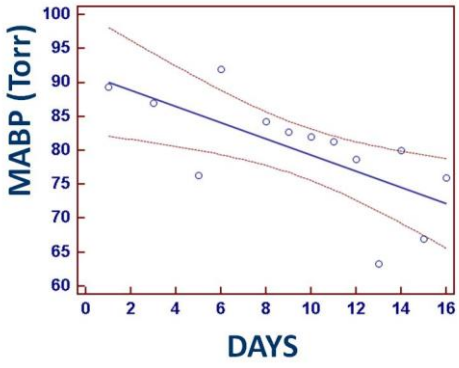

Figure 12 The linear inverse regression of mean arterial blood pressure (MABP) values plotted against the corresponding days of assessment. The regression is depicted as a straight line segment with 13 open circles indicating the accepted measurements, as one data point was excluded after being identified as an outlier. The two orange dashed lines represent the 95% confidence interval.
The corresponding regression equation was:

$$TPVR\ (Torr\ l^{-1}\ min) = 26.14 - 0.77\ (days) \quad (13)$$

Equation (13) showed a P = 0.007, so reaching the statistical significance. Similarly to HR, the HMW did not show any statistically significant trend in both linear and quadratic HMW-versus-days regression analyses.

Nevertheless, this relationship is illustrated in Figure 14 for completeness. Figure 15 shows the quadratic regression of the rate–pressure product (RPP) values plotted against the corresponding days. The RPP–days regression equation was as follows:

$$RPP\ (b\ min^{-1}\ Torr) = 7418.9 - 229.1(days) + 17.9(days)^2 \quad (14)$$

Table III – Clinical-functional variables

N (16)	SO2 %	BT °C	PEF l min-1	HAG kg
Mean	97.1	35.7	513.7	44.0
±SD	1.1	0.4	21.2	2.1
VI%	1.13	1.12	4.13	4.77

SO2: oxygen percentage in saturation of arterial blood; BT: body temperature measured at tympanic level; PEF: peak of the maximum expiratory flow; HAG: handgrip maximum effort. VI: variability index as SD percentage on Mean. N is the total number of considered measurements to calculate their average value (Mean) together with its standard deviation (±SD).

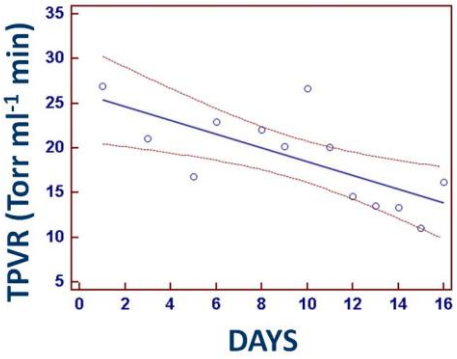

Figure 13 The linear regression of total peripheral vascular resistance (TPVR) values plotted against the corresponding days of assessment. The regression includes 13 open circles representing the accepted measurements, as one data point was excluded after being identified as an outlier. The two orange dashed lines represent the 95% confidence interval.

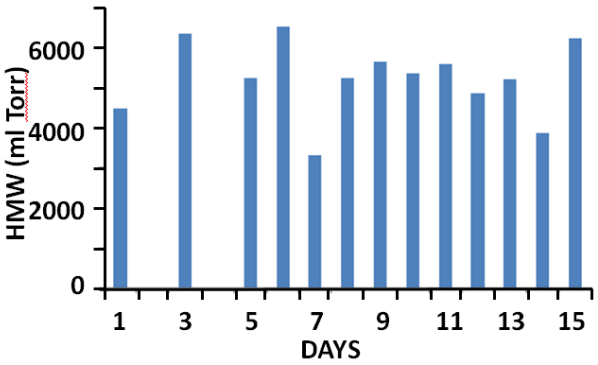

Figure 14 The column histogram represents the heart's mechanical work (HMW) for each of the 13 selected days of kayak paddling. As described in the Methods section, data from days 2 and 4 were excluded from the analysis, while day 16 was identified as an outlier.

Equation (14) showed a "P" value of 0.023, indicating statistical significance. The vertex of the parabola was negative and located at approximately 6.4 days on the x-axis, corresponding to between the 12th and 13th days from the start of the measurements. As shown in Figure 16, the relationship between heart mechanical efficiency (HME) and days was also modelled using a quadratic regression, expressed as:

$$HME\ (b^{-1}\ min\ ml) = 0.586 + 0.068(days) - 0.0045(days)^2 \quad (15)$$

Equation (15) yielded a "P" value of 0.071which almost reached statistical significance. However, the vertex of the parabola was positive and positioned at approximately 7.5 days on the x-axis, corresponding to between the 14th and 15th days from the beginning of the measurements.
Figure 17 illustrates the quadratic regression of SO2% values plotted against the corresponding measurement days. The SO2%–days regression equation was:

$$SO2\ (\%) = 96.43 + 0.39\ (days) - 0.03\ (days)^2 \quad (16)$$

Equation (16) showed a "P" value of 0.011, indicating statistical significance. The vertex of the parabola was positive and located at approximately 6.5 days on the x-axis, corresponding to between the 12th and 13th days from the start of data collection. Figure 17 shows the linear regression of BT values plotted against days. The corresponding regression equation was:

$$BT\ (°C) = 36.143 - 0.055\ (days) \quad (17)$$

Equation (17) yielded a "P" value of 0.0002, indicating a highly significant statistical relationship. Figure 18 shows the quadratic regression of HAG values plotted against days. The corresponding regression equation was:

$$HAG\ (kg) = 40.391 + 1.024\ (days) - 0.052\ (days)^2 \quad (18)$$

Equation (19) yielded a "P" value of 0.06, which—similar to the SV versus days relationship—did not reach the threshold for statistical significance, although it was very close to the 0.05 cut-off adopted in this study. The parabola had a positive vertex located at approximately 9.8 days on the x-axis, corresponding to between the 19th and 20th days from the start of measurements. Regarding the relationships of peak expiratory flow (PEF) as well as the other two assessed variables which were the urine specific gravity (USG) and rate of perceived exertion (RPE) variations across the selected days of kayak paddling, both the linear and quadratic regression analyses were far from reaching statistical significance. Therefore, these daily variations were represented graphically as histograms, shown in Figures 20, 21 and 22.

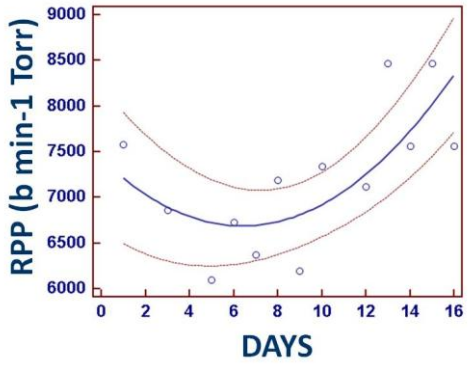

Figure 15 The quadratic regression of the rate–pressure product (RPP) values plotted against the corresponding assessment days, represented as a segment of a parabolic curve. Thirteen open circles indicate the accepted measurements, as one data point was excluded as an outlier. The orange dashed lines represent the 95% confidence interval.

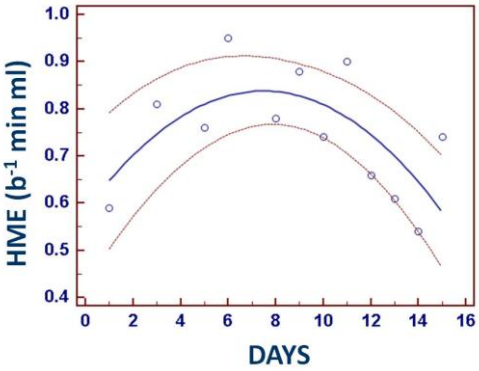

Figure 16 The quadratic regression of heart mechanical efficiency (HME) values plotted against the corresponding assessment days, represented as a segment of a parabolic curve. Twelve open circles indicate the accepted measurements, as two data points were excluded as outliers. The two orange dashed lines represent the 95% confidence interval.

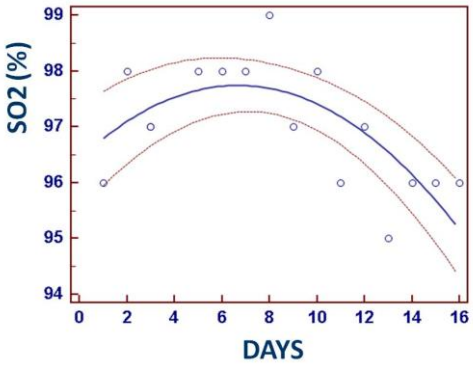

Figure 17 The quadratic regression of the arterial blood oxygen saturation in percentage values (SO2) versus corresponding days of their assessment represented as a segment of a parabolic curve with 15 empty circles concerning the 16 accepted measurements since one of those considered was excluded resulting as an outlier value. The two orange dashed lines represent 95% confidence interval.

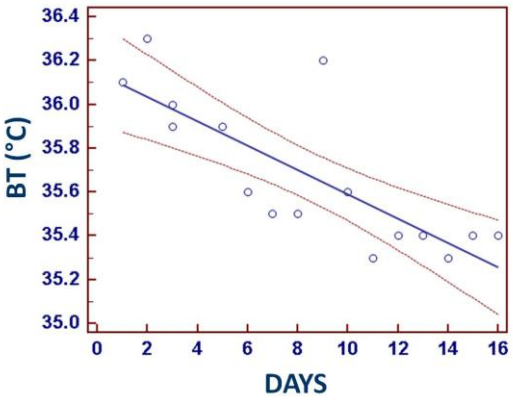

Figure 18 shows the linear regression of body temperature (BT) values plotted against the 16 corresponding assessment days. Sixteen open circles represent the accepted measurements, while the two orange dashed lines indicate the 95% confidence interval.

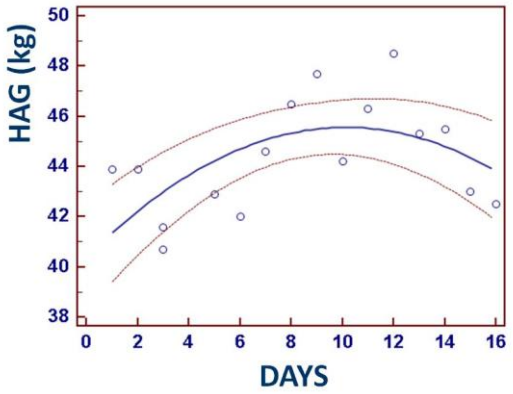

Figure 19 shows the quadratic regression of handgrip maximum effort (HAG) values plotted against the 16 corresponding assessment days, represented as a segment of a parabolic curve. Sixteen open circles indicate the accepted measurements, while the two orange dashed lines represent the 95% confidence interval.

3 DISCUSSION

To obtain daily resting values for blood flow variables—whose mean values are reported in the Tables I and II—a custom-built impedance cardiograph was employed in this study. This device had previously been validated by comparing its measurements with those obtained from commercially available ICG systems considered the gold standard for cardiovascular assessments [19]. To further enhance the reliability of the present results, Table IV shows the mean values of TFI, SV, CO, EVI, and TPVR—cardiovascular variables measured almost with the E-Physio tool—visually correlated with corresponding resting-state values obtained in two independent experiments that used two well-established commercial ICG instruments. As illustrated in the table, except for EVI, the four other variables assessed with the E-Physio tool fall within an intermediate range between the values obtained using the two commercial devices: the BioZ ICG Monitor

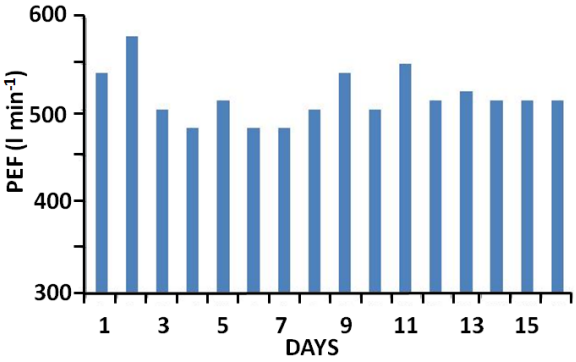

Figure 20 shows the column histogram representing the peak expiratory flow (PEF) values for each of the 16 selected days of the athlete's kayak paddling.

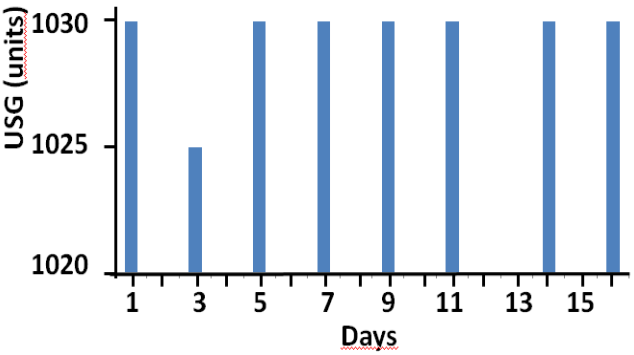

Figure 21 shows the column histogram representing the urine specific gravity (USG) values. Due to practical difficulties in recording this parameter nightly before bedtime, the athlete was instructed to perform the measurements every two days. However, the assessment planned for day 13 could not be completed and was postponed to day 14, with the final measurement taken on day 16.

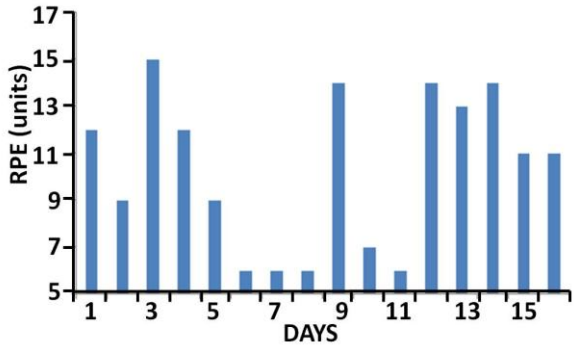

Figure 22 shows the column histogram representing the rate of perceived exertion (RPE) values for each of the 16 selected days of kayak paddling.

Table IV – Comparison from different ICG devices

Variables	BioZ ICG (2006)	E-Physio (actual)	Niccomo™ (2025)
TFI(Ω)	33.1	32.5	29.1
SVI(ml/m^2)	33.0	37.0	50.2
COI(l/min/m^2)	2.3	3.2	3.3
EVI(Ω/s)	1.16	1.89	1.38
PVR(Torr/ml/min)	33.3	25.8	24.7

(CardioDynamics, San Diego, California, USA) [20] and the Niccomo™ (Medis Medizintechnik, Ilmenau, Germany) [21]. This finding supports the view that the variables measured with the E-Physio tool can be regarded as reasonably reliable, despite the higher LVMCI (EVI) value compared to the other two methods. This discrepancy may be attributed to quantitative and qualitative differences among the three groups of subjects included in the comparison. Of primary importance, however, is that—as shown in Equation (11)—these experimental results revealed several cardiovascular adaptations which, over the 30-day observation period, collectively led in this kayaker to a predicted linear increase in resting CO of approximately 65 *ml min^{-1}* per day. As is well known, both SV and HR are the variables that determine CO through their mathematical product. It must therefore be considered that SV, in turn, depends on central (cardiac) determinants—namely, the thoracic fluid index (TFI) and ejection velocity index (EVI)—as well as on peripheral (vascular) determinants such as ventricular afterload, expressed as total peripheral vascular resistance (TPVR).

The experimental data predicted a linear increase in SV of about 0.61 *ml day^{-1}*, corresponding to a rate of increase of 1.09 % *day^{-1}*. However, this latter result requires further confirmation, as its current statistical significance was marginal (P = 0.06). However, the ICG-derived reciprocal indicator of LVPL, i.e. Zt, or the thoracic fluid index (TFI), showed a significant linear increase of approximately 0.21 *Ω day^{-1}*. This finding indicates a corresponding reduction in LVPL, the heterometric (central) variable influencing SV. In contrast, this trend was opposed by the concurrent linear increase in the EVI, the ICG-derived indicator of LVMC—that is, the homeometric (central) factor determining SV—which increased by about 26 *mΩ s^{-1} day^{-1}*.

When the daily rate of variation of LVPL and LVMC was expressed as a percentage of their respective intercept values on the ordinate axis (see Equations 9 and 10), the results indicated a change of –0.75% *day^{-1}* for LVPL and +1.83 % *day^{-1}* for LVMC. These findings suggest that, in our athlete, prolonged kayak paddling induced a progressive increase in resting SV, not primarily through an enhancement of ventricular preload, but rather through a predominant contribution from myocardial contractility. This pattern indicates a sympathetic dominance in the autonomic control of cardiac function, as the daily percentage rate of increase in SV more closely matched that of LVMC than that of LVPL. In previous work by Sheykhlouvand et al. [22], well-trained sprint kayakers underwent incremental cardiopulmonary tests on a kayak ergometer before and after eight weeks of high-intensity interval training performed on the same device. Following the training period, these authors reported that, in elite kayakers, the increase in LVMC did not coincide with a parallel rise in LVPL. Specifically, they found that resting SV increased significantly due to enhanced ventricular contractility, as evidenced by an elevated left ventricular ejection fraction (LVEF), while the increase in SV exceeded that observed for LVPL. Therefore, consistent with the findings of the present study, those authors concluded that in trained kayakers, an improvement in myocardial contractility can enhance SV even in the absence of an increase in LVPL, with this adaptation being primarily attributable to an increase in LVEF. In this context, it is noteworthy that in the previously reported post-trip echocardiographic evaluation at rest [1], our kayaker exhibited a 4% increase in LVEF compared with the pre-trip value. Furthermore, Bertozzi et al. [23] observed that high-intensity kayak sprints predominantly affect the kinematics of the shoulders, trunk, and hips during paddling, while exerting a much smaller influence on lower limb motion. This finding is consistent with a reduced contribution of the calf muscle pump to venous return during paddling, resulting in a comparatively lower preload stimulus. Consequently, a limited functional adaptation of LVPL, even when measured at rest, could reasonably be expected in our kayaker. Moreover, based on Equation (8), which describes the relationship between SV and days of observation, the predicted increase in resting SV after 30 days of navigation was +32.6%. This value closely matches the +31.2% increase previously measured at rest by echocardiography at the end of the kayak cruise [1]. With regard to the potential influence of the peripheral heterometric vascular factor—namely, total peripheral vascular resistance (TPVR)—on SV and, consequently, on CO, it is noteworthy that TPVR exhibited a negative and highly significant linear regression with respect to trip duration, as shown in Equation (13). Specifically, TPVR decreased by approximately 0.77 *Torr l^{-1} min day^{-1}* (Figure 13). This finding resulted in a clear inverse CO–TPVR relationship, illustrated in Figure 23, which likely contributed to the observed time-dependent increase in cardiac output. Indeed, the daily self-recorded measurements of these two variables, collected each evening by the athlete after setting up camp, revealed a strong inverse dependence of CO on TPVR. As demonstrated by the linear regression depicted in Figure 23 and described by Equation (19), this relationship predicted an increase in CO of approximately 170 ml min^{-1} for each unit decrease in TPVR, with a very high level of statistical significance (P < 0.0001).

$$CO\ (l\ min^{-1}) = 7.64 - 0.17\ (Torr\ l^{-1}\ min) \quad (19)$$

It has been well established that regular aerobic exercise training—such as that performed by this kayaker—promotes skeletal muscle angiogenesis [24], leading to an increase in muscle capillarization [25]. From a purely hemodynamic perspective, an increase in muscle capillarization corresponds to an expansion of the hydraulic conduits within striated muscles, which are arranged in parallel, resulting in a consequent decrease in TPVR [26]. This is precisely what was observed in our kayaker at the end of the cruise. In a recent study involving healthy adults performing the 6-minute walk test (6MWT) [27], a submaximal-intensity exercise, a negative association was found between the distance covered and TPVR.

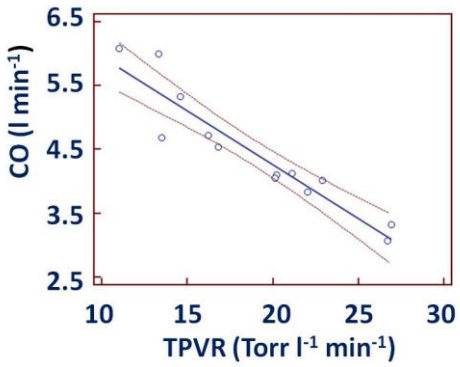

Figure 23 shows the inverse linear regression of cardiac output (CO) values against the corresponding total peripheral vascular resistance (TPVR) values. Thirteen open circles represent the 14 accepted measurements, since one data point was excluded as an outlier. The two orange dashed lines indicate the 95% confidence interval.

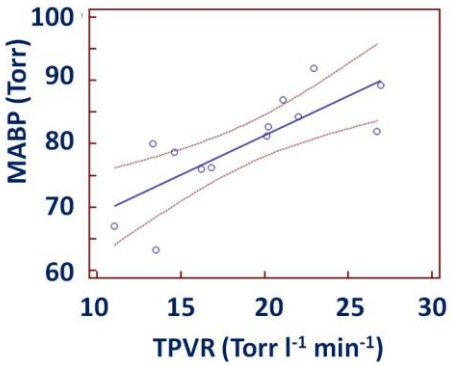

Figure 24 The linear regression of mean arterial blood pressure (MABP) against total peripheral vascular resistance (TPVR). Thirteen open circles represent the accepted measurements, while one data point was excluded as an outlier. The two orange dashed lines indicate the 95% confidence interval.

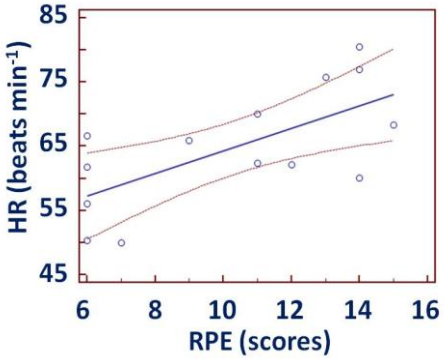

Figure 25 shows the linear regression of heart rate (HR) against the corresponding ratings of perceived exertion (RPE). Fourteen open circles represent the accepted measurements, while the two orange dashed lines indicate the 95% confidence interval

At the same time, a moderate-to-strong positive correlation emerged between 6MWT distance and oxygen consumption. Therefore, it can be hypothesized that the prolonged, submaximal exercise performed by our kayaker—since it produced a progressive and significant reduction in TPVR—may also have led to an improvement in aerobic capacity. This hypothesis is strongly supported by the previous observation [1] that this athlete's maximal oxygen consumption, measured during the cardiopulmonary exercise test conducted after the kayak expedition, was approximately 13% higher than the value recorded during the pre-expedition test. As expected [26], the Figure 24 illustrates the kayaker's daily decrease in TPVR, which was accompanied by a parallel reduction in MABP, quantified by Equation (20) as approximately -1.3 Torr for each unit decrease in TPVR (P = 0.001).

$$MABP\ (Torr) = 56.44 + 1.24\ (Torr\ l^{-1}\ min \tag{20}$$

The effect described in Equation (20) was not chronotropically compensated by increases in HR, as the two here chosen kind of regressions for MABP on HR—namely linear and quadratic—here chosen, did not reach statistical significance.

Conversely, during the coastal trip, the kayaker's HR at rest was strongly and directly correlated with his RPE. The relationship between HR and RPE scores is illustrated in Figure 25 as a linear regression line, described by the following equation:

$$HR\ (b\ min^{-1}) = 46.77 + 1.75\ (RPE\ scores) \tag{21}$$

Equation (21) indicates a predicted increase of nearly 2 beats per minute for each unit increase in RPE score (P = 0.0091). The absence of any statistically significant relationship between HR and MABP reasonably excludes modulatory influences from carotid and aortic baroreflex activity [28]. This finding supports the interpretation that the observed increases in HR are better explained by the classical Cannon–Bard physiological principle [29], whereby sympathetic chronotropic activation of the heart arises from persistent painful sensations associated with increased physical effort [30], as clearly shown in Figure 25 and Equation (21). Furthermore, from a strictly clinical perspective, the results of this experiment suggest that continuous sea kayaking may elicit an antihypertensive effect of non-pharmacological origin. In this experiment, it was also possible to collect data on the mechanical work and efficiency adaptations of the athlete's heart over the month of daily resting measurements, which he self-performed each evening. As shown in Table II, the mean HMW value reached a VI% approaching 20%, while the histogram in Figure 25 clearly shows a positively skewed distribution, with more than 50% of the HMW values ranging between 5000 and 6500 *Torr ml*. As shown in Figure 26, the higher HMW values are located in the right half of the graph, suggesting that these elevated values occurred during the second half of the kayak journey.

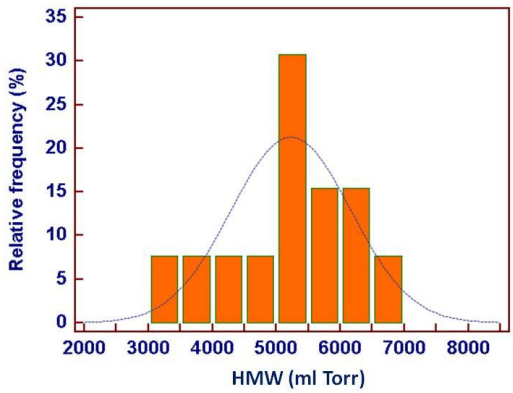

Figure 26 The columns in the histogram represent the relative frequency distribution of the athlete's heart mechanical work (HMW) values measured daily during the last 30 days of navigation. Although a positive skewness of the descriptive distribution is evident, the D'Agostino–Pearson test indicates that the data follow a normal (parametric) distribution (P = 0.544).

This observation indicates that during the final two weeks of paddling, the mechanical work performed by the heart was slightly greater than during the first two weeks. The asymmetrical distribution of HMW values therefore accounts for the relatively high VI% associated with their mean. An interesting finding emerges from the observation that, during the second half of the trip, the workload imposed on the athlete's heart resulted in a markedly high and progressively increasing oxidative energy cost. This is illustrated in Figure 15, which shows the squared regression of RPP versus days, as well as in the corresponding Equation (14) that generated the graph. As expected at this stage, the trend of HME over time was nearly the inverse of the previous one. Indeed, as shown in Figure 16 and described by Equation (15), the HME–days relationship is represented by a parabolic curve with its vertex directed upward, corresponding to an abscissa value around day 15—approximately two weeks after the start of measurements. This clearly indicates that, from the beginning of the third week until its end, the mechanical efficiency of the heart decreased in a quadratic manner, returning to values similar to those recorded at the start of the trip when the journey ended. Unfortunately, the parabolic regression equation (15) for HME versus days did not reach a full up statistical significance since a P-value of 0.071. To better contextualize the behaviour of the mechanical and energetic variables of our resting athlete's heart during the final days of his coastal cruise, Figure 27 (bottom panel) shows a graph in which the curve derived from the RPP–days relationship is superimposed with the corresponding temporally matched HME–days curve. The top panel of Figure 26 presents a graph adapted from the study by Evans and Matsuoka, published in "The Journal of Physiology" (London, 1915) [31]. In their experiment on an isolated heart from a small mammal (59 g), conducted under constant blood pressure and temperature but with varying cardiac output, they demonstrated that as the mechanical work of the heart (abscissa, expressed in $kg\ m^{-1}\ h^{-1}$) increased linearly, oxygen consumption (solid curve) rose exponentially. The geometry of this curve closely resembles that of the RPP curve for our athlete (bottom panel), particularly during the second half of the observation period. Correspondingly, the mechanical efficiency of the isolated heart (dotted curve in the top graph) followed a parabolic trend with a positive vertex, analogous to the HME behaviour observed in the kayaker's data. Notably, in both cases—approximately halfway through the maximum workload of the isolated heart in the first graph and at midway through the total duration of the athlete's monitoring period—the mechanical efficiency of each heart began to decline from its respective maximum value, corresponding to the vertex of the parabola. The data reported by Evans and Matsuoka [31] could undoubtedly be regarded as a milestone in understanding the bioenergetics underlying the mechanical activity of the mammalian heart [32]. In that study, the authors—consistent with the conclusions of Patterson et al. [33]—

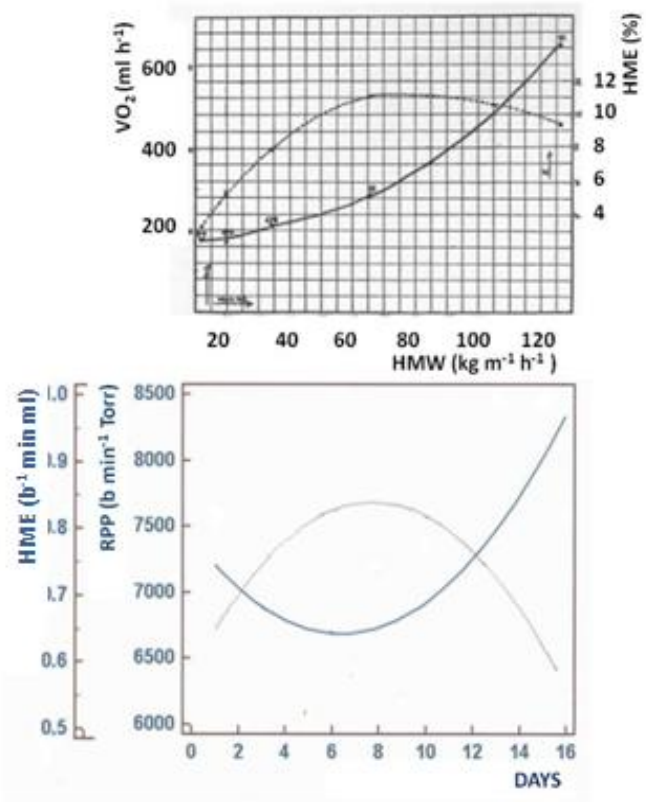

Figure 27 Top panel: Graphical representation of oxygen consumption (VO_2, solid curve) and mechanical efficiency (HME, dotted curve) as functions of the linearly increasing heart mechanical work (HMW) in an isolated small mammalian heart. Bottom panel: Graphical representation of the rate–pressure product (RPP, blue solid curve) as an index of myocardial oxygen consumption, and of the heart's mechanical efficiency (HME, black solid curve), both plotted as functions of the progressive days of the athlete's paddling activity.

demonstrated that under very high cardiac workloads, signs of myocardial fatigue emerge, manifested by an increased energy cost (i.e., higher VO_2 consumption) and a consequent reduction in mechanical efficiency. Translating these experimental findings from ex vivo animal preparations to the indirect measurements of cardiac mechanics obtained from this kayaker, it can be inferred that, during the final weeks of his circumnavigation of the island of Sardinia, the athlete may have developed a state of cardiac fatigue. Interestingly, the HAG/days curve shown in Figure 19 predicted that as the days of the cruise progressed, the maximum handgrip force—measured at rest—gradually increased during the early phase of the voyage, peaking around the tenth day of observation, and subsequently declined toward the end of the journey. This progressive reduction in HAG during the final part of the cruise seemsto temporally coincide with both the ascending limb of the quadratic RPP/days curve (representing the increasing energetic cost of cardiac work) and the descending limb of the HME/days quadratic curve (indicating reduced mechanical efficiency of cardiac performance). Taken together, these three concomitant trends suggest the development of a generalized fatigue condition in our kayaker during the latter stages of his daily paddling routine. This hypothesis is further supported by the persistently high values of urinary specific gravity, averaging 1.030 (as shown in Figure 21), which point to a state of pronounced dehydration. Indeed, in previous studies dehydration has been shown to impair both the mechanical efficiency of the cardiac cycle [34] and the force transmission capacity of striated muscles [35]. In addition, the quadratic relationship between SO2% and days ($P = 0.011$; see Figure 16 and Equation 16) revealed a clear and progressive decline beginning approximately in the second half of the monitoring period, further supporting the hypothesis of cumulative physiological fatigue during the final phase of the coastal cruise. Similarly, the progressive reduction in body temperature (BT/days) should not be overlooked, as shown in Figure 18 and described by the corresponding regression Equation (17). According to this equation, the rate of decrease in BT was approximately –0.027 $^{\circ}C$ per day. By 30th day of navigation, this corresponded to a total decline of about –0.82 $^{\circ}C$, indicating that body temperature decreased from an initial value of 36.14 $^{\circ}C$ (the intercept of the regression line at the start of the experiment) to 35.32 °C at the end of the observation period—representing an overall reduction of roughly 1 $^{\circ}C$. During the athlete's navigation, data recorded by the HOBO device indicated that the average minimum environmental temperatures ranged between 8 °C and 11 °C, with the lowest values occurring during nighttime hours when the kayaker was resting on the beach inside his tent and performing self-measurements. Relative humidity averaged 70–75%, with higher peaks at night and in the early morning. Therefore, the observed trend in BT can reasonably be interpreted as a physiological response consistent with the environmental conditions encountered during the expedition. It is noteworthy that, as previously reported, blood flow to the fingers decreases during cold exposure, and this phenomenon appears to result from cold-induced increases in blood viscosity rather than from vasoconstriction [36]. Consequently, it is possible that the progressive reduction in BT observed during the trip also lowered the temperature of the fingers, through which SO2% was measured. The resulting increase in blood viscosity could have contributed to a reduction in local SO2%, particularly during the latter part of the trip (as shown by the SO2%/days curve in Figure 17). This effect might, in turn, have been transmitted retrogradely to the vascular, muscular, and ligamentous structures responsible for hand contractile activity, thereby contributing to a decline in mechanical efficiency. Furthermore, it was previously reported [1] that, by the end of his kayaking expedition, this athlete had lost 3.5 kg of body weight, of which 1.9 kg corresponded to free fat mass (FFM). This reduction included a loss of total body water (TBW), which had decreased by 1.5 kg at the end of the trip. Considering that the other components of FFM—namely internal organs (approximately 25%), bones (approximately 15%), and mineral reserves (approximately 15%)—are unlikely to undergo substantial reductions in a healthy, physically active individual, the remaining 0.4 kg decrease in FFM can reasonably be attributed to a loss of skeletal muscle mass (MM). This reduction in MM likely contributed to the observed decrease in maximal force output during the HAG tests performed towards the end of the kayaking journey. It is therefore not surprising that, as shown in the bar graph in Figure 22, depicting the athlete's (RPE) every two days, the mean RPE value during the final eight measurements was approximately 20% higher than that recorded during the first eight. Finally, although the variability index (VI) of the mean daily self-assessed PEF measured by the kayaker was only 4% (as shown in Table III), the column histogram in Figure 20 suggests that, after the first three days of observation, this variable showed a slight but noticeable reduction—approximately −4%—over the remaining days of the trip. This may indicate the presence of a subclinical dysfunction of the upper airways that developed gradually during the athlete's prolonged performance at sea. Indeed, exercising in a challenging environment such as the marine setting—characterized by high humidity, fluctuating temperatures, and prolonged exposure to wind and salt—may disrupt the delicate water–salt balance of the bronchial mucosa, potentially leading to respiratory impairment [37]. Such an effect appears to have occurred in our long-distance kayaker, possibly exacerbated by a state of borderline dehydration. However, recent studies [38] have suggested that sea spray aerosols (SSAs) contain bioactive compounds derived from marine algae that can modulate cellular processes relevant to human health. Specifically, exposure of human bronchial epithelial cells to natural SSA samples has been shown to activate gene clusters associated with anti-inflammatory and anti-tumor responses. These findings therefore support the notion that our kayaker was exposed to potentially beneficial effects during his prolonged coastal journey [2].

4 STUDY LIMITATIONS

The main limitation of this study is that it was conducted on a single subject. However, implementing an experimental protocol involving several kayakers simultaneously undertaking the same course as our athlete is currently impractical for this research team. Another limitation is that the statistical regressions of some key variables—SV, HME, and HAG—yielded "P" values ranging from 0.055 to 0.071, thus not achieving full statistical significance. Considering the observed temporal trends of these variables, it is reasonable to assume that this outcome might have differed had data collection included the first 10 days of navigation. To verify this hypothesis, the authors plan to repeat the experiment on the same athlete under conditions involving a substantially longer navigation period.

5 CONCLUSION

The experimental results presented here can reasonably be regarded as the first comprehensive dataset describing the physiological adjustments and adaptations of multiple organs and body systems involved in a long-duration kayaking performance. In this context, the findings of the present study—together with those previously obtained from the same kayaker [1]—make a significant and original contribution to our understanding of the functional model of athletes engaged in prolonged paddling activities.

REFERENCES

[1] Tocco F., Massidda M., Ghiani G., Palmas M., Ruggiu M., Velluzzi F., Solinas R., Masala A., Fois A., Melis L., Manuello Bertetto A., Dell'Osa A.H., Cerina A., Cappagli C., Melis S., Loi V., Marcello R. and Concu A., Biomechanical and cardiometabolic changes in skilled kayaker after 41 days of cruising around the island of Sardinia: a case study (part 1). *International Journal of Mechanics and Control*, Vol. 25, No. 02, pp. 113-119, 2024.

[2] Tocco F., Mattana D.V., Solinas R., Velluzzi F., Usai P., Fois A., Melis L., Bianco P., Serra C., Manuello Bertetto A., Dell'Osa A.H., Pereira A.F., Cerina A., Loviselli L., Marcello R., Melis S. and Concu A., Cardiometabolic benefits from a coastal sailing in a radical cystectomy patient remotely controlled by an internet of thing mechatronic tool: a case study. *International Journal of Mechanics and Control*, Vol. 24, No. 02, pp. 39-61, 2023.

[3] Campagna M., Lecca L.I., Velluzzi F., Serra C., Bianco P., Manuello Bertetto A., Dell'Osa A.H., Fanni B., De Pau A., Fois A., Melis L., Kalb A., Marcello R., Melis S., Concu A. and Tocco F., A mechatronic simulator of an aircraft cockpit to study, by a virtual flight test, cardiovascular fitness in airline pilots banned to fly since covid-19 lockdown. *International Journal of Mechanics and Control*, Vol. 23, No. 02, pp. 85-99, 2022.

[4] Saito K., Hishiki Y. and Takahashi H., Validation of two automatic devices, Omron HEM-6232T and HEM-6181, for self-measurement of blood pressure at the wrist according to the ANSI/AAMI/ISO 81060-2:2013 protocol and the European Society of Hypertension International Protocol revision 2010. *Vasc Health Risk Manag*, Vol. 15, pp. 47-55, 2019.

[5] Buyse G.M., Rummey C., Meier T., Leinonen M., Voit T., McDonald C.M. and Mayer O.H.J., Home-Based Monitoring of Pulmonary Function in Patients with Duchenne Muscular Dystroph. *Neuromuscul Dis*, Vol. 5, No. 4, pp. 419-430, 2018.

[6] Daneshparvar A., Hemmatinafar M., Salesi M., Rezaei R., Imanian B. and Pirmohammadi S., The effect of acute beetroot juice consumption prior to climbing on lower-body isokinetic and isometric strength, aerobic power, and muscle soreness among mountain climbers. *J Int Soc Sports Nutr*, Vol. 22, No. 1, pp. 2502656, 2025.

[7] Leppänen T., Kainulainen S., Korkalainen H., Sillanmäki S., Kulkas A., Töyräs J. and Nikkonen S., Pulse Oximetry: The Working Principle, Signal Formation, and Applications. *Adv Exp Med Biol*, Vol. 1384, pp. 205-218, 2022.

[8] Nobel J.J., Infrared ear thermometry. *Pediatr Emerg Care*, Vol. 8, No. 1, pp. 54-58, 1992.

[9] Wu W.C., Concu A., Solinas R., Meloni L., Manuello-Bertetto A., Fois A., Loviselli A., Deledda A. and Velluzzi F., Metabolic power and energy cost of mechanical work carried out by a sailor engaged in a solo ocean race: a case study. *International Journal of Mechanics and Control*, Vol. 19, No. 02, pp. 19-32, 2018.

[10] Marongiu E., Crisafulli A., Ghiani G., Olla S., Roberto S., Pinna M., Pusceddu M., Palazzolo M., Sanna I., Concu A. and Tocco F., Cardiovascular Responses during free-diving in the sea. *Int J Sports Med*, Vol. 36, pp. 297-301, 2015.

[11] Tocco F., Solinas R., Velluzzi F., Massidda M., Mattana D.V., Fois A., Melis L., Manuello Bertetto A., Bonisoli E.†, Venturini S., Bianco P., Dell'Osa A.H., Pereira A.F., Melis S., Cerina A., Loviselli L., Marcello R. and Concu A., A mechatronic tool for revealing inverse relationships among heart's stroke volume and head's linear acceleration induced by moored boats rolling in elderly sailors with unchanged body sizes: a non-drug anti-hypertensive advantage?. *International Journal of Mechanics and Control*, Vol. 25, No. 01, pp.133-142, 2024.

[12] Dell'Osa A.H., Fois A., Cerina A., Pili F., Manuello Bertetto A., Bellomi G., Palmas M., Ruggiu M., Melis S., Tocco F. and Concu A., Impedance cardiography assessment during body immersion in a high concentrated water solution of magnesium chloride simulating space microgravity: a pilot study. *J Phys: Conf. Ser.* 3014, 012006, 2025.

[13] Manuello Bertetto A.,Tocco F., Bellomi G., Mulargia L., Ruggiu M., Palmas M., Massidda M., Ghiani G., Velluzzi F., Melis S., Fois A., Dell'Osa A.H., Cerina A., Bertelli U., Carta M.G., Bianco P.R. and Concu A., Cardiovascular and metabolic engagement after an endurance race in pilots driving motorboats electrically powered by green Energy. *International Journal of Mechanics and Control*, Vol. 26, No. 01, pp. 221-230, 2025.

[14] Bernstein D.P., A new stroke volume equation for thoracic electrical bioimpedance: theory and rationale. *Crit Care Med*, Vol. 14, No. 10, pp.904-909, 1986.

[15] Sramek B.B., Noninvasive technique for measurement of cardiac output by means of electrical impedance. *Proc. of the 5th International Conference on Electrical Bioimpedance*, Tokyo, Japan, pp. 39-42, 1981.

[16] Dash R.R., Samanta P., Das S., Jena A., Panda B., Parida B.B. and Mishra J., Heart Rate Variability in Unexplained Syncope Patients Versus Healthy Controls: A Comparative Study. *Cureus*, Vol. 15, No. 7, pp. e41370, 2023.

[17] Borg G. and Dahlstrom H., A case study of perceived exertion during a work test. *Acta Soc Med Ups*, Vol. 67, pp. 91-93, 1962.

[18] Keyser R.E., Andres F.F., Wojta D.M. and Gullett S.L., Variations in cardiovascular response accompanying differences in arm-cranking rate. *Arch Phys Med Rehabil*, Vol. 69, No. 11, pp. 941-945, 1988.

[19] Tocco F., Crisafulli A., Marongiu E., Milia R., Kalb A. and Concu A. (2012). A portable device to assess underwater changes of cardiodynamic variables by impedance cardiography. *J Phys: Conf. Ser.* 407, 012026, 2012.

[20] Packer M., Abraham W.T., Mehra M.R. *et al.*, Utility of impedance cardiography for the identification of short-term risk of clinical decompensation in stable patients with chronic heart failure. *J Am Coll Cardiol*, Vol. 47, No. 11, pp. 2245-2252, 2006.

[21] Domino B., Wlochacz A., Maciorowska M. *et al.*, Impaired cardiovascular hemodynamics in patients hospitalized with COVID-19 pneumonia. *J Clin Med*, Vol. 14, pp. 1806, 2025.

[22] Sheykhlouvand M., Arazi H., Astorino T.A. and Suzuki K., Effects of a new form of resistance-type high-intensity interval training on cardiac structure, hemodynamics, and physiological and performance adaptations in well-trained kayak sprint athletes. *Front Physiol*, Vol. 13, pp, 850768, 2022.

[23] Bertozzi F., Porcelli S., Marzorati M., Pilotto A.M., Galli M., Sforza C. and Zago M. Whole-body kinematics during a simulated sprint in flat-water kayakers. *Eur J Sport Sci*, Vol. 22, No. 6, pp. 817-825, 2022.

[24] Rodrigues L.F.,Rocha Avila Pelozin B., da Silva Junior N.D. *et al.*, Angiotensin II promotes skeletal muscle angiogenesis induced by volume-dependent aerobic exercise training: effects on miRNAs-27a/b and oxidant-antioxidant balance. *Antioxidants (Basel)*, Vol. 11, No. 4, pp. 651, 2022.

[25] Liu Y., Christensen P.M., Hellsten Y. and Gliemann L., Effects of exercise training intensity and duration on skeletal muscle capillarization in healthy subjects: a meta-analysis. *Med Sci Sports Exerc*, Vol. 54, No. 10, pp. 1714-1728, 2022.

[26] Berne R.M. and Levy M.N., *Cardiovascular Physiology*. 5th edition, McGraw-Hill, New York, USA, 1986.

[27] Singhasoot S.,Srijunto W.,Werasirirat P., Namsawang J.,Chaovalit S. and Muanjai P., Associations between 6-min walk distance and cardiopulmonary parameter in non-obese older adults: An observational study. *Respir Med*, Vol. 236, pp. 107912, 2025.

[28] Concu A., Cardiovascular adjustments during exercise: points and counterpoints. Eds. Crisafulli A. and Concu A*., New insight into cardiovascular apparatus during exercise. Physiological and physio-pathological aspects*. Research Signipost, Kerala, India, pp. 61-84, 2007.

[29] Cannon W.B., The James-Lange theory of emotions: a critical examination and an alternative theory. *Am J Psychol*, Vol. 39, pp. 106-124, 1927.

[30] Glenn E.W., and Goetz S.M.M., Applying Evolutionary Thinking to the Study of Emotion. *Behav Sci*, Vol. 3, pp. 388–407, 2013.

[31] Evans C.L. and Matsuoka Y., The effect of various mechanical conditions on the gaseous metabolism and efficiency of the mammalian heart. *J Physiol*, Vol. 49, No. 5, pp. 378-405, 1915.

[32] Margaria R. and De Caro L., *Fisiologia Umana*. Vol. 1, Ed. Vallardi, Milano, Italy, pp. 13, 1967.

[33] Patterson S.W., Piper H. and Starling E.H.J., The regulation of the heart beat. *J Physiol*, Vol. 48, No. 6, pp. 465-513, 1914.

[34] Lax D., Eicher M. and Goldberg S.J., Mild dehydration induces echocardiographic signs of mitral valve prolapse in healthy females with prior normal cardiac findings. *Am Heart J*, Vol. 124, No. 6, pp. 1533-40, 1992.

[35] De Moura R.C., De Moura Costa C., Ferreira C.P. *et al.*, Hydration assessment and physical performance of mountain bike cyclists in competition in a hot environment. *Sci Rep*, Vol. 15, No. 1, pp. 21183, 2025.

[36] Scotto G.,Miniaci M.C., Silipo F. and Scotto P., Reduction of cutaneous blood flow in cold fingers. *Boll Soc Ital Biol Sper*, Vol. 74, No. 3-4, pp. 35-41, 1998.

[37] Karamaoun C., Haut B., Blain G., Bernard A., Daussin F., Dekerle J., Bougault V. and Mauroy B.J., Is airway damage during physical exercise related to airway dehydration: Inputs from a computational model. *J Appl Physiol*, Vol. 132, No. 4, pp. 1031-1040, 2022.

[38] Liu Z., Van Acker E., De Rijcke M., Van Nieuwerburgh F., Janssen C. and Asselman J., Exploring seasonal dynamics of sea spray aerosol bioactivity: Insights into molecular effects on human bronchial epithelial cells, *Environ Int*, Vol. 195 pp. 109255, 2025.